Int. J. Electrochem. Sci., 15 **(2020)** 1072 – 1081, doi: 10.20964/2020.02.03

International Journal of
ELECTROCHEMICAL
SCIENCE
www.electrochemsci.org

Short Communication

Corrosion Behavior Study of Aluminum Alloy 7075-T6 and 2A12-T6 Joints Prepared Using Friction Stir Welding

Defeng Zhang[*], *Jun Xia, Qiuguo Yang, Tianhao Wei, Lijie Gong, Siyue She*

School Of Materials Science and Engineering, Southwest Petroleum University, Chengdu 610500, China
[*]E-mail: 574285778@qq.com

Received: 12 September 2019 / *Accepted:* 13 November 2019 / *Published:* 31 December 2019

The corrosion resistance of FSW welded joints of 6mm-thick dissimilar 2A12 and 7075 aviation aluminum alloy was investigated. It was concluded that the 7075 aluminum alloy was more resistant to intergranular corrosion than 2A12 aluminum alloy, and when the 7075 aluminum alloy was the advancing side (AS) material, the intergranular corrosion resistance of the WNZ of the dissimilar aluminum alloy FSW joint was better than the 2A12 aluminum alloy. But the polarization curve and AC impedance diagram of the electrochemical corrosion test shown that the corrosion resistance of the WNZ of the FSW joint was better than that of the 2A12 aluminum alloy on the advancing side (AS) when the 7075 aluminum alloy was on the advancing side (AS). And when the 7075 aluminum alloy was the advancing side material, the corrosion resistance of each region of the joint was: 2A12BM>HAZ+TMAZ(RS)>WNZ>7075BM>HAZ+TMAZ(AS).

Keywords: FSW; Dissimilar aluminum alloy; Intergranular corrosion; Electrochemical measurement

1. INTRODUCTION

2A12 aluminum alloy was a commonly used Al-Cu-Mg aluminum alloy that could be strengthened by heat-treating. 2A12 aluminum alloy contained many copper elements, which greatly improved its strength, hardness and mechanical processing properties. It was widely used in the fields of aerospace industry and high-speed trains. 7075 aluminum alloy belonged to Al-Zn-Cu-Mg series alloy, in which the zinc was the main alloy element. It was representative of super hard aluminum alloy in 7000 series. 7075 had good properties in wear resistance and corrosion resistance. It was easy to be processed and could be strengthened by heat treatment. Therefore, 7075 aluminum alloy was widely used in aerospace, fixture, mold processing and other fields.7075 was especially used for aircraft structures, which required excellent corrosion resistance and high strength. Such as propellers, rockets, aircraft landing gear and skins on the wings etc. We knew that both of 2A12 and 7075 aluminum applied

in aerospace. So studied the welding of the dissimilar Al-ally that must be profound in aircraft structure. But the joint would inevitable product many defects during the traditional fusion welding process. In 1991， Friction stir welding invented by W. M. Thomas in the British Welding Institute (TWI) [1]. FSW was a new type of solid-phase joining technology, which was connected by the thermal coupling between the stirring tool with high speed rotation and feeding motion and the material to be welded [2-3]. And Friction stir welding had special advantages for the welding of dissimilar materials and was widely applied to the welding of different materials [4-8]. Such as [9] studied on Electrochemical and Surface about Friction Stir Welding Joints of Aluminum-Copper Dissimilar Alloys. At present, FSW technology had been successfully applied in aerospace, shipbuilding, high-speed trains and other fields [10-11]. Up to now, scientific research workers had been making extensive research and analysis on the friction stir welding of 2000 series and 7000 series aluminum alloys at home and abroad [12-16]. For instance, in [17] the effect of heat treatment and welding condition on the corrosion behavior of 7075 T6 Al alloy without material contribution has been investigated. And the result of the corrosion test shown that the corrosion rates were very similar for both the base metal and welding. Similarly， in [18] studied on the effect of surface roughness on pitting corrosion of 2A12 aluminum alloy. In that paper, the researcher concluded that 2A12 aluminum alloy exhibited lower corrosion susceptibility and lower pit growth rate as the decreasing of surface roughness. However, there was few report about the friction stir welding of dissimilar aluminum alloys of the 2000 series and 7000 series. In this paper, 6mm thick 2A12 and 7075 dissimilar aluminum alloys were used for friction stir welding, and the corrosion resistance of the welded joints was analyzed and studied. This FSW technology for aluminum alloys had considerable high engineering application value and scientific significance in the aerospace field.

2. EXPERIMENTAL

2.1 Material Preparation

Table 1. Chemical composition of the 7075-T6 and 2A12-T6 aluminum alloys (wt.%).

Alloys	Si	Fe	Mn	Cu	Ni	Zn	Mg	Al
2A12-T6	≤0.50	≤0.50	≤0.30~0.90	3.8~4.9	≤0.10	≤0.30	1.2~1.8	Bal
7075-T6	≤0.40	≤0.50	≤0.30	1.2~2.0	--	5.1~6.1	2.1~2.9	Bal

The welding test plates of 2A12T6-7075T6 dissimilar aluminum alloy used in this paper was welded by the friction stir welding machine, which was independently invented by Northeast University. And the shape of the stirring head of the friction stir welding machine was conical. This experiment mainly studied the corrosion resistance of joints when different aluminum alloy materials placed on the advancing side. Therefore, except for the materials on the advancing side, the other welding process parameters were consistent. The size of all plates were both of 500mm×110mm×6mm. Through consulting the experimental parameters of friction stir welding of aluminum alloy, the FSW welding parameter setting was finally selected as shown in Table 2.

Table 2. The welding parameters.

Sample code	Rotational speed (ω)rpm	Traverse speed (v)mm min^{-1}	Tilt angle (°)	Plunge depth (mm)
7075-T6(AS)	800	40	0.3	0.2
2A12-T6(AS)	800	40	0.3	0.2

2.2. Intergranular Corrosion Test

For intergranular corrosion (IGC) test of joint referred to GB/T 7998-2005 "Method for determination of intergranular corrosion of aluminum alloys". The intergranular corrosion samples were processed to ensure that the weld was in the middle of the intergranular corrosion sample. And the sample sizes were shown in Fig. 1. The sides of the sample were polished and mirrored under a trickle water using 400 mesh, 600 mesh, 800 mesh, 1000 mesh, 1200 mesh, 2000 mesh, 2500 mesh, 3000 mesh, 5000 mesh and 7000 mesh abrasive paper in turn. And the joint was divided into different regions. As shown in Fig. 2, which was a schematic cross-sectional view of the weld seam of the welded joint. We divided that into four areas: A, B, C and D are the base metal (BM); Heat affected zone (HAZ); Thermo-Mechanically Affected Zone (TMAZ) and the weld nugget zone (WNZ) [19-20], respectively. And a, b, c were divided into a advancing side and a retreating side (the left side of the weld nugget as advancing side and the right side is retreating side).

The pre-treatment cleaning solution was configured to be 10% NaOH solution and 24% HNO_3 solution respectively. And the samples were sequentially subjected to alkali washing, acid washing and water washing, and dried for later using. An intergranular corrosion solution was prepared. And its composition was 3% NaCl + 10 mL / L H_2O_2. We poured the intergranular corrosion solution into a 500 ml jar and hung the sample into the bottle. When the sample was completely immersed in the intergranular corrosion solution and sealed with silica gel. Then we would place the jar in an XF/HWHS-150L thermostat at 35℃ ±2℃ for 6 hours.

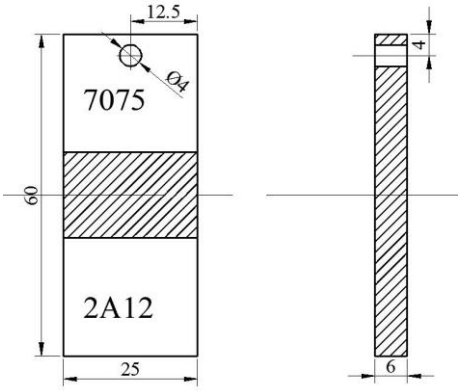

Figure 1. Intergranular corrosion test specimen

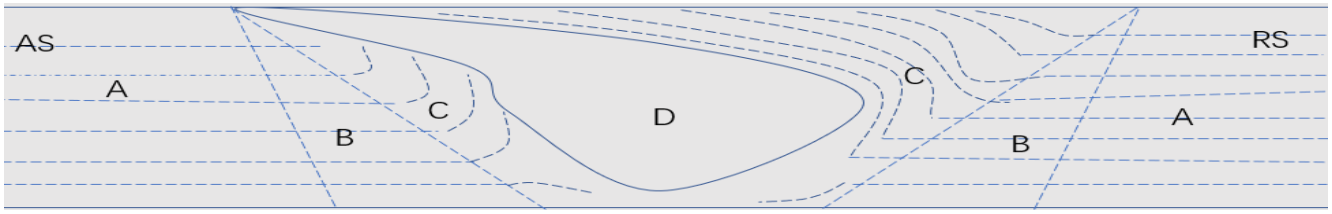

Figure 2. Schematic diagram of cross section of FSW joint
A-BM, B-HAZ, C-TMAZ, D-WNZ

When the corrosion experiment was completed, the sample was taken out. Then the sample was washed by deionized water and dried. After the corrosion, the corroded specimen was cut perpendicular to the weld seam in different areas by wire cutting. These specimens were polished to a mirror surface by abrasive paper. The intergranular corrosion process and mechanism of dissimilar aluminum alloy FSW joints were analyzed by SEM observation and EDS elemental analysis of the corroded samples. Finally, the expansion of intergranular corrosion was observed and the depth was measured under the VMD-P3008 optical metallographic microscope.

2.3 Electrochemical test

The electrochemical test of the joint adopted CS150H electrochemical workstation manufactured by Wuhan CorrTest Instruments Corp., Ltd. In the electrochemical corrosion test, the sample was cut at the base metal of 7075 and 2A12; WNZ; AS-TMAZ+AS-HAZ (AS-advancing side); RS-TMAZ+RS-TMAZ (RS-retreating side), respectively. The size of all samples were 60 mm×12 mm×6 mm. Then, these samples were polished and then ultrasonically washed with acetone, alcohol, and deionized water for five minutes in turn. Finally, the samples were blown dry by a hair dryer, and used paraffin to seal the part other than the surface to be tested. The etching solution was a 3.5% NaCl solution. The test temperature was 35 ±2°C. The polarization curve of the joint was measured by the scanning method. The scanning speed was 1 mV/s and the potential measurement range was -2.3 V-1.0 V.

3. RESULTS AND DISCUSSION

3.1 Intergranular corrosion behavior

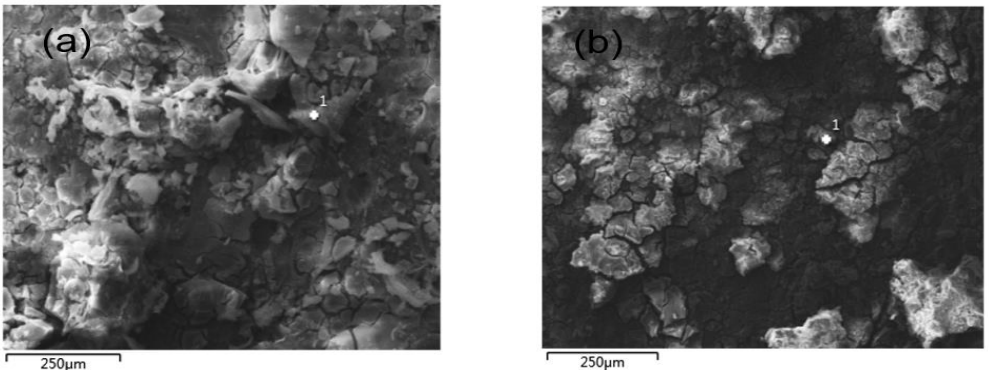

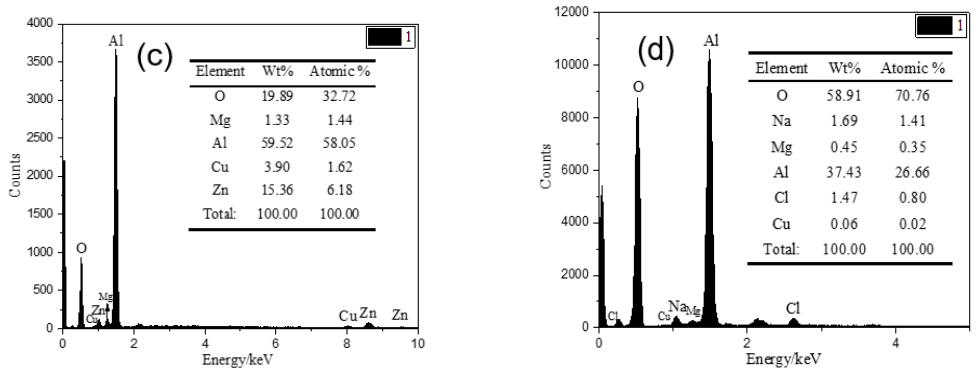

Figure 3. (a) the SEM of 7075-BM, (b) the SEM of 2A12-BM
(c) the EDS of 7075-BM, (d) the EDS of 2A12-BM

Fig. 3 (a), (c) was the SEM morphology and EDS analysis of intergranular corrosion of 7075 aluminum alloy base material, respectively. The SEM image showed that the corrosion products in this area were thicker, with fewer pitting pits and fewer corrosion cracks than base material of 2A12. (b), (d) was the SEM morphology and EDS analysis of the intergranular corrosion of 2A12 aluminum alloy base material, respectively. In the SEM image, the corrosion morphology was irregular at the point of taking. It was possible that the second phase reacted to form corrosion products that stacked on the surface of the sample and seriously cracking and falling occurred.

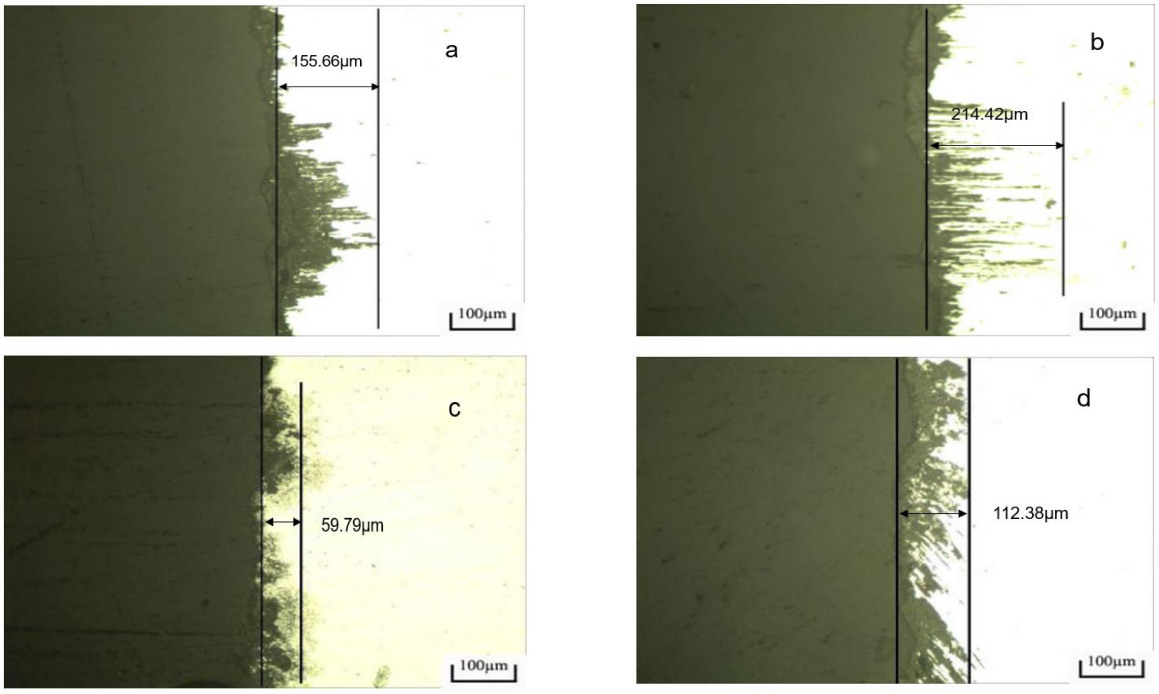

Figure 4. (a) IGC-morphology of 7075-BM, (b) IGC-morphology of 2A12-BM
(c) IGC-morphology of WNZ (7075 on AS), (d) IGC-morphology of WNZ (2A12 on AS)

Looking at the EDS analysis chart, the content of O and Cl were obviously changed, the Al content was reduced by 10%, which indicated that the corrosion in this area was severe. Comparing the

EDS diagrams of (c) and (d), it can be seen that the Al content of the 2A12 aluminum alloy base material was reduced by 10%, while the Al content of the 7075aluminum alloy base material was just decreased by 1.4%. The result suggested that the intergranular corrosion resistance of 7075 aluminum alloy was better than 2A12 aluminum alloy.

Fig 4(a) and 4(b) shown the IGC propagation morphology of the 7075aluminum alloy and the 2A12 aluminum alloy base material, respectively. Comparing 4(a) and (b) the two figures shown that the maximum corrosion depth of the 7075aluminum alloy was 155.66μm, while the maximum corrosion depth of the 2A12 aluminum alloy base material was 214.42μm. Both of them were grade 4 corrosion. As shown the figure 4(a) and 4(b) of IGC-morphology, the intergranular corrosion of the aluminum alloy base material was very obvious. But the corrosion degree of the 2A12 aluminum alloy was more severe than that of the 7075. So we considered that the 7075aluminum alloy was more resistant to intergranular corrosion than the 2A12. The result of the analysis was consistent with conclusion from Figure 3. According to the previous analysis, we knew that 2A12 aluminum alloy contained more Cu element than 7075 aluminum alloy. And the addition of Cu element led to the continuous precipitation of Cu-rich $CuAl_2$ phase aggregate at the grain boundary, which would lead to the formation of Cu-lean zone at the grain boundary. In the Cu-lean zone, $CuAl_2$ was the cathode and the grain boundary of the Cu-lean zone was the anode, which formed corrosion battery and caused intergranular corrosion. The more Cu elements in the aluminum alloy and the more the precipitation of the second phase, the more severe the intergranular corrosion was. So the above result was obtained. Fig 4(c)and 4(d) were the corrosion-expanded morphologies of the WNZ when the advancing side material was 7075 and 2A12, respectively. Both of the grain boundary corrosion profile could be clearly seen in the two diagrams. The intergranular corrosion was easy to develop along the grain boundary. And the IGC morphology was not uniform in the transverse direction. Comparing the intergranular corrosion extension morphology of the joint WNZ with different materials on the advancing side, the longitudinal expansion depth of intergranular corrosion was similar. But when 7075 was placed on the advancing side, the grain boundary transverse corrosion depth of WNZ was 59.79μm. While the corrosion depth of WNZ of joints with 2A12 on the advancing side was 112.38μm. The former was grade3 corrosion and the latter was grade 4 corrosion. Because the higher the intergranular corrosion level, the more severe IGC was. The weld nugget zone of dissimilar aluminum alloy FSW joint had better intergranular corrosion resistance when 7075 was placed on the advancing side.

Comparing the IGC of the base metal (BM) and the weld nugget zone (WNZ), it was concluded that the WNZ had much better intergranular corrosion resistance than the 7075-BM and 2A12-BM. It was possible that the dynamic recrystallization of the weld nugget zone made the grain in the WNZ finer and more uniform than the BM, which resulted in better resistance to intergranular corrosion in the WNZ than the BM. Because the larger the grain size, the more second phase particles precipitated at the grain boundary, and the more susceptive of IGC at the grain boundary was. And the large size of the grains facilitated the development of the corrosive medium through the continuous grain boundary to the deep metal layer [21]. For the dissimilar aluminum alloy FSW joint in this study, the microstructure of WNZ was fine equiaxed crystal, so the susceptibility to IGC was the smallest, while the microstructure of BM was coarsened by the heating cycle and the susceptibility to IGC was the largest. When the 7075 aluminum alloy was placed on the advancing side, the IGC resistance of the joint weld nugget zone was

better than the 2A12 on the advancing side. This might be due to the fact that when 7075 was the advancing side material, which was good for the weld material moving to backwards of the stirring needle. So that the material of the weld nugget region was more uniformly mixed. Thus, the dynamic recrystallization of the weld nugget zone under the action of the stirring needle generates less tissue defects, which resulted in better resistance to intergranular corrosion of the weld nugget region when the 7075aluminum alloy placed on the advancing side than when the 2A12 as the advancing side. The less defects and more closely bonded between the grains, the less susceptive of IGC. Finally, we had come to the conclusion that the resistance of IGC of WNZ of dissimilar Al-ally FSW joint was better when 7075 Al-ally as the advancing side material. And the WNZ had the better resistance of IGC than BM.

3.2. Electrochemical test analysis

Table 3. Electrochemical parameters of the weld nugget zone of FSW joint

Material of the advancing side	Self-corrosion current ($\mu A/cm^2$)	Self-corrosion potential (mV)	Passivation interval (mV)
7075	35.6	-1108	361
2A12	80.9	-1151	334

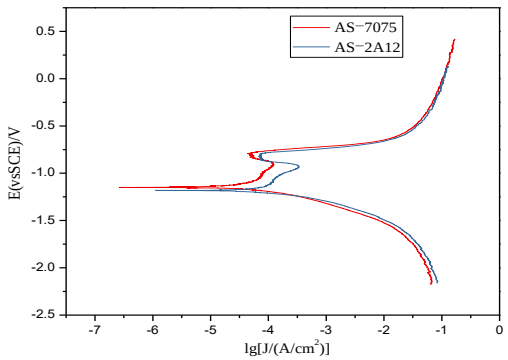

Figure 5. Potentiodynamic polarization curves of the WNZ with different AS material (samples in in 3.5 wt. % NaCl solution at 35±0.5 °C and the Scanning rate was 1mV/ s)

When 7075 aluminum alloy and 2A12 aluminum alloy were taken as the advancing side material respectively, the dynamic potential polarization curves of WNZ of dissimilar Al-ally FSW joint weld was shown as fig.5. The dynamic potential polarization curves of the WNZ were analyzed to obtain their self-corrosion potential and self-corrosion current density. The results were shown in Table 3. From the test results, when the 7075 aluminum alloy took as the advancing side of the FSW dissimilar aluminum alloy weld, the self-corrosion potential of the WNZ was -1108.2 mV, which moved to the positive direction compared with -1151.0 mV when 2A12 aluminum alloy took as the advancing side of joint. And when the 7075 aluminum alloy was on the advancing side, the self-corrosion current of the WNZ was 35.6μA/cm^2. That self-corrosion current density of the WNZ was less than 2A12 when it was the advancing-side material, which was 80.9μA/cm^2. In [22] the researcher had come to a conclusion that the more positive self-corrosion potential and the lower self-corrosion current density, the better

corrosion resistance was. The above result was due to the fact that the 7075 aluminum alloy took placed on the advancing side, the material was mainly mixed by the 2A12 aluminum alloy moved to the advancing side of the joint and achieved to mix in the WNZ. While the 2A12 aluminum alloy was placed on the advancing side, which mixed mainly by the 7075 aluminum alloy. However, when 7075 aluminum alloy took placed on the retreating side, the flow property of moving to the advancing side was not as good as the 2A12 aluminum alloy on the retreating side. Therefore, when the 2A12 aluminum alloy was the advancing side material, which was not conducive to the migration and mixing of the weld material. So when 2A12 aluminum alloy on the advancing side, which resulted in uneven mixing of the weld material. In [23] they suggested that the uneven mixing of the weld material at WNZ might increase the tendency of the WNZ to appear defects as tunnel hole. And these defects would reduce the corrosion resistance of the WNZ. We had the same point about that. Finally, we had concluded that when 7075 Al-alloy was the advancing side material of FSW dissimilar aluminum alloy joint. The corrosion resistance of the joint weld nugget zone (WNZ) was better than that 2A12 Al-alloy as the advancing side material. This result was consistent with the range of passivation interval, which shown in table 3.

Table 4. Electrochemical parameters of different regions of FSW joints when 7075 aluminum alloy took placed on the advancing side

Different joint areas	Self-corrosion current ($\mu A/cm^2$)	Self-corrosion potential (mV)
7075-BM	74.4	-1161
HAZ+TMAZ(AS)	97.5	-1164
WNZ	35.6	-1108
HAZ+TMAZ(RS)	19.1	-1104
2A12-BM	10.9	-1096

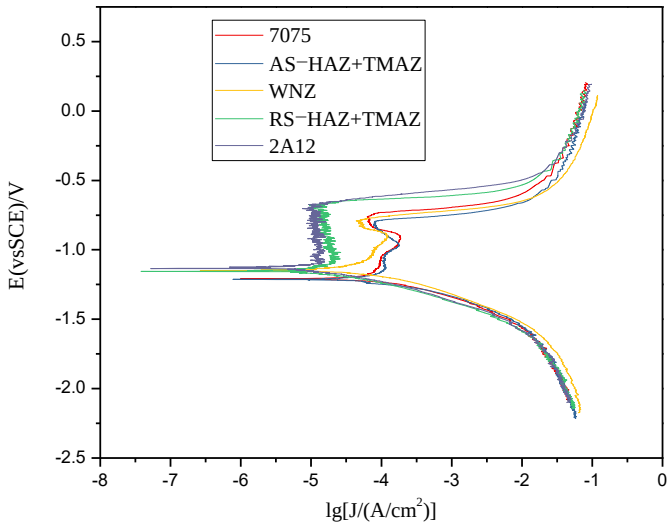

Figure 6. Polarization curves of different regions of the FSW joint when 7075 Al-alloy on the AS (samples in in 3.5 wt. % NaCl solution at 35±0.5 °C and the Scanning rate was 1mV/ s)

In fig. 6, we could see the dynamic potential curves of 7075/2A12 dissimilar aluminum alloy FSW joint weld in various regions when 7075 Al-alloy was the advancing side material. Table4 listed the self-corrosion potential and self-corrosion current density in each region of the weld when 7075 Al-alloy as the advancing side material. Researchers at home and abroad agreed that self-corrosion current density and self-corrosion potential could reflect the corrosion resistance of materials [24-25]. They believed that the magnitude of the self-corrosion current reflected the corrosion resistance of the material. The smaller the self-corrosion current density, the more corrosion resistant the material was. The positive and negative deviation of self-corrosion potential reflected the tendency of corrosion of material, and the more positive the potential, the less obvious the tendency of corrosion. According to the self-corrosion current density and self-corrosion potential of each part of the welded joint when the 7075 Al-alloy placed on the advancing side in Table 4. Finally, we concluded that the corrosion resistance performance of each part of the FSW joint was;2A12> HAZ +TMAZ(RS)> WNZ>7075>HAZ+TMAZ (AS).

The above result might be due to the fact that the size of the second phase particles of the 2A12 aluminum alloy base material was much smaller than the second phase particles size of the 7075 aluminum alloy base material. According to the Table1, we knew that the content of Cu and Zn in 7075 aluminum alloy was more than 2A12 aluminum alloy. And both elements would form micro-cells with the matrix [26-27]. The more micro-cells formed in the alloy, the more serious the corrosion was. So 2A12 aluminum alloy was more resistant to corrosion than 7075 aluminum alloy. The corrosion rate of the WZN was fast. That might be due to the dynamic recrystallization and grain refinement in the weld nugget zone, which improved the corrosion resistance of this area less than the large amount of residual stress in this area, which damaged its performance. Moreover, the stirring in the WNZ increased the grain boundary energy, which further increased the corrosion susceptibility of the WNZ. The corrosion rate of the HAZ+TMAZ mixed zone on the retreating side was lower than the WNZ. Because the self-corrosion current density only reflected the pre-electrochemical corrosion. In the later stage of corrosion, the coarsened second phase of the mixed zone would corrode and further promote corrosion. The corrosion rate of the mixed zone would be larger than the WNZ.

4. CONCLUSIONS

In this paper, 6mm thick 2A12 and 7075 aluminum alloy sheets were studied and analyzed for the corrosion properties of FSW joints of different advancing side materials. And the following conclusions were obtained:

(1) Through the analysis of intergranular corrosion, we obtained that the intergranular corrosion resistance of 7075 aluminum alloy base material was better than that of 2A12 aluminum alloy base material. And when the 2A12 and 7075 aluminum alloys were respectively on the advancing side, through the studied of the intergranular corrosion propagation in the weld nugget zone, We concluded that the intergranular corrosion resistance of the joint weld nugget zone was better when the 7075 aluminum alloy was on the advancing side. And the WNZ exhibited better corrosion resistance than BM.

(2) Electrochemical corrosion of 2A12/7075 dissimilar aluminum alloy FSW joint shown that the corrosion resistance of the FSW joint weld nugget of the 7075 aluminum alloy was better than that

the 2A12 aluminum alloy as the FSW joint on the advancing side. And when 7075 was the advancing side material. The corrosion resistance performance of each region of the dissimilar aluminum alloy FSW joint was;2A12BM>HAZ+TMAZ(RS)>7075BM>WNZ>HAZ+TMAZ(AS)

References

1. W.M. Thomas, E.D. Nicholas, J.C. Needham, M.G. Murch, P. Temple-Smith and C. J. Dawes: 'Friction stir butt welding', GB patent no. 9125978.8, 1991.
2. A. Kostka, R.S. Coelho, J. dos Santos, A.R. Pyzalla, *Scr. Mater. Sci*., 60 (2009) 953.
3. B.C. Liechty, B.W. Webb, *International Journal of Machine Tools & Manufacture. Sci*., 48 (2008) 1474.
4. Z.X. Zhao, H.M. Liang, Y. Zhao, K. Yan, *J. Mater. Eng. Perform. Sci.,*27 (2018) 1777.
5. Hamed Jamshidi Aval, *Materials and Design. Sci,*67 (2015) 413.
6. R. Padmanaban, V. Ratna Kishore, V. Balusamy, *Procedia Eng.Sci.,*97 (2014) 854.
7. Gianluca D'Urso, Claudio Giardini, Sergio LoreWNZi, Marina Cabrini, Tommaso Pastore, *Procedia Eng.Sci.,* 207 (2017) 591.
8. Ravikumar. S, SeshagiriRao. V, Pranesh.R. V, *Procedia Mater. Sci. Sci.,*5 (2014) 1726.
9. Neetesh Soni, Y.C. Yang, Adepu Kumar, C.H. Yin, L. Liu, Ambrish Singh, Y.H. Lin, *Int. J. Electrochem. Sci.,* 14 (2019) 8949.
10. G.H. Luan, D.L. Guo, Q. Guan, T.C. Zhang, *Aeronautical Manufacturing Technology*. 10 (2002) 43.
11. D.F. Chen, T.H. Zhang, F.D. Zhang, X.F. Fang, X.S. Liu, *Welding Technology*, 44 (2015) 74.
12. Chaitanya Sharma, Dheerendra Kumar Dwivedi, Pradeep Kumar, *Materials and Design. Sci.,*36 (2012) 379.
13. Y.B. Song, X.Q. Yang, L. Cui, X.P. Hou, Z.K. Shen, Y. Xu, *Materials and Design*, 55 (2014) 9.
14. P. Cavaliere, R. Nobile, F.W. Panella, A. Squillace, *International Journal of Machine Tools & Manufacture. Sci.,* 46 (2006) 588.
15. B. Han, Y.X. Huang, S.X. Lv, L. Wan, J.C. Feng, G.S. Fu, *Materials and Design*, 51 (2013) 25.
16. H.Y. Wu, L. Xing, Y.H. Chen, C.P. Huang, *Heat Treat. Met*. 36 (2011) 90.
17. V.A. Arizmendi-Salgado, S.A. Serna, A. Torres-Islas, R. Soto-Espitia, P. Althuzer, *Int. J. Electrochem. Sci.,* 14 (2019) 8243.
18. W.M. Tian, B.X. Chao, X.Y. Xiong, Z.Y. Li, *Int. J. Electrochem. Sci.,* 13 (2018) 3107.
19. H.H. Hu, G.H, Luan, P. Cai, Locomotive & Rolling Stock Technology, 4 (2006) 4.
20. W.G. Li, *Research on Friction Stir Welding Process and Microstructure and Properties of Dissimilar Aluminum Alloys Joints*, Jiangsu University of Science and Technology, 2016, Jiangsu, China.
21. Amjad Saleh El-Amoush, *Mater. Chem. Phys. Sci.,*126 (2011) 607.
22. L.J. Li, J.X. He, J.L. Lei, W.T. Xu, X. Jing, X.T. Ou, S.M. Wu, N.B. Li, S.T. Zhang, *Surf. Coat. Technol. Sci.,*279 (2015) 72.
23. Y.D. Zhao, *Electrochemical Corrosion Behavior of Friction Stir Welding Weld of Aluminum Alloy,* Dalian Jiaotong University, 2008, Liaoning, China.
24. P. Bala Srinivasan, K.S. Arora, W. Dietzel, S. Pandey, M.K. Schaper, *J. Alloys Compd. Sci.,* 492 (2010) 631.
25. S.G. Wang, Y. Huang, L. Zhao, *Rare Metal Materials and Engineering. Sci.,*47(2018) 1973.
26. Ali Davoodi, Zohreh Esfahani, Madjid Sarvghad, *Corros. Sci.Sci.,* 107 (2016) 133.
27. Sunil Sinhmar, Dheerendra Kumar Dwivedi, *Corros. Sci.Sci.,*133 (2018) 25.